

Intermolecular interactions involving C-H bonds. 3. Structure and energetics of the interaction between CH<sub>4</sub> and CN<sup>-</sup>.

Juan J. Novoa<sup>a</sup> and Myung-Hwan Whangbo

Department of Chemistry, North Carolina State University  
Raleigh, North Carolina 27695-8204

Jack M. Williams

Chemistry and Materials Science Divisions,  
Argonne National Laboratory, Argonne, Illinois 60439

<sup>a</sup> On sabbatical leave from Departamento de Quimica Fisica, Facultad de Quimica, Universidad de Barcelona, 08028-Barcelona (Spain)

Abstracts

Patent Cleared by  
Patent Department, ANL

RELEASE AUTHORIZED BY  
Technical Publications Services

Date 4/14/91

024

David R. Hamrin

Technical Information Services, ANL

On the basis of SCF and single reference MP2 calculations, the full potential energy surface of the interaction between CH<sub>4</sub> and CN<sup>-</sup> was studied using extended basis sets of up to near Hartree-Fock limit quality. Colinear arrangements C-N<sup>-</sup>...H-CH<sub>3</sub> and N-C<sup>-</sup>...H-CH<sub>3</sub> are found to be the only two energy minima. The binding energies of these two structures are calculated to be 2.5 and 2.1 kcal/mol, respectively, at the MP2 level. The full vibrational analyses of the two structures show a red shift of about 30 cm<sup>-1</sup> for the  $\nu_s$  C-H stretching.

The submitted manuscript has been authored by a contractor of the U. S. Government under contract No. W-31-109-ENG-38. Accordingly, the U. S. Government retains a nonexclusive, royalty-free license to publish or reproduce the published form of this contribution, or allow others to do so, for U. S. Government purposes.

OCT 14 1991

OS MASTER

## **DISCLAIMER**

This report was prepared as an account of work sponsored by an agency of the United States Government. Neither the United States Government nor any agency thereof, nor any of their employees, make any warranty, express or implied, or assumes any legal liability or responsibility for the accuracy, completeness, or usefulness of any information, apparatus, product, or process disclosed, or represents that its use would not infringe privately owned rights. Reference herein to any specific commercial product, process, or service by trade name, trademark, manufacturer, or otherwise does not necessarily constitute or imply its endorsement, recommendation, or favoring by the United States Government or any agency thereof. The views and opinions of authors expressed herein do not necessarily state or reflect those of the United States Government or any agency thereof.

## **DISCLAIMER**

**Portions of this document may be illegible  
in electronic image products. Images are  
produced from the best available original  
document.**

## Introduction

In the present work, we examine the interaction between  $\text{CN}^-$  and  $\text{CH}_4$  on the basis of ab initio calculations to evaluate the nature and magnitude of the  $\text{C-N} \cdots \text{H-CH}_3$  and  $\text{N-C} \cdots \text{H-CH}_3$  contact interactions. Since a C-H bond is less polar than F-H and O-H bonds, the  $\text{C-N} \cdots \text{H-CH}_3$  and  $\text{N-C} \cdots \text{H-CH}_3$  interactions are expected to be weaker than the  $\text{C-N} \cdots \text{H-F}$  and  $\text{C-N} \cdots \text{H-OH}$  interactions recently studied by Lee [1]. Our calculations on  $\text{C-N} \cdots \text{H-CH}_3$  and  $\text{N-C} \cdots \text{H-CH}_3$  could provide relevant information on the nature and strength of the interactions that C-H bonds of organic donor molecules make with counter anions containing  $\text{CN}^-$  groups in organic donor salts (e.g.,  $\text{C-N} \cdots \text{H-C}$  and  $\text{N-C} \cdots \text{H-C}$  contact interactions) [2]. No experimental data are available for the energetics of the  $\text{C-N} \cdots \text{H-C}$  and  $\text{N-C} \cdots \text{H-C}$  contact interactions in organic salts. So far, neither computational nor experimental studies have been carried out on the  $\text{CN}^-$ -methane complex.

In our study of the  $\text{CN}^-$ -methane complex, we perform SCF and single reference MP2 calculations to determine its potential energy surface. Since the HOMO-LUMO separations in the  $\text{CN}^-$  and  $\text{CH}_4$  fragments are large, single reference MP2 calculations are expected to give a good description of the  $\text{CN}^-$ -methane complex. In addition, according to the binding energy calculations of the  $\text{CN}^-$ -HF and  $\text{CN}^-$ - $\text{H}_2\text{O}$  complexes using a triple zeta plus double polarization plus diffuse s and p basis set [1], both the SCF and single reference MP2 methods give results in good agreement with those obtained from singles and doubles CI as well as singles and doubles coupled cluster calculations. Therefore, the present SCF and single reference MP2

calculations are expected to provide reliable estimates of the binding energy of the CN<sup>-</sup>...methane complex.

### Computational details

To study the potential energy surface of the CN<sup>-</sup>...methane complex, we perform calculations on the three geometrical arrangements shown in 1-3. The C-N<sup>-</sup>...H-CH<sub>3</sub> (1) and N-C<sup>-</sup>...H-CH<sub>3</sub> (2) arrangements are models for studying the C-N<sup>-</sup>...H-C and N-C<sup>-</sup>...H-C contact interactions, respectively. The CN<sup>-</sup>...methane arrangement 3 is used to examine the energetics associated with the C-H...anion contact change from 1 to 2.

In order to accurately describe anionic systems, use of large enough basis sets with diffuse functions are needed [3]. At the same time, a precise description of intermolecular interactions requires the use of at least double zeta plus double polarization basis sets [4]. One basis set satisfying both requirements is the 6-31++G(2d,2p) basis implemented in GAUSSIAN-86 [5]. Use of this basis set and the MP2 method for the potential energy surface calculations is too demanding computationally, so that we carried out the potential energy calculations with the standard 6-31++G(d,p) basis set at the SCF level. After identifying the characteristics of the surface, precise calculations, including reoptimization of the geometry, were performed with more extended basis sets at the single reference MP2 level on some regions of the potential energy surface. All computations were carried out with the GAUSSIAN-86 program [5].

## Results and discussion

### 1) Potential energy surface of the CN<sup>-</sup>...methane interaction

For the CN<sup>-</sup>...HF and CN<sup>-</sup>...H<sub>2</sub>O complexes, the SCF method gives geometries and binding energies very close to those obtained with the MP2 method [1]. It is noted that the SCF results in Ref. 1 are closer to experiment and are within 1 kcal/mol of the experimental values. Therefore, we expect to obtain a reasonable picture of the nature of the CN<sup>-</sup>...methane interaction by carrying out SCF calculations with the 6-31++G(d,p) basis set. The potential energy surface for 1-3, obtained as a function of the two parameters defining the interaction between the frozen fragments [6], is shown in Figure 1. This surface is characterized by two minima and a transition state linking them: one minimum is found for the CN<sup>-</sup>...H-CH<sub>3</sub> arrangement (1) at  $r_{NH} = 2.652 \text{ \AA}$  and  $\theta = 0^\circ$ , another minimum corresponds to the NC<sup>-</sup>...H-CH<sub>3</sub> arrangement (2) at  $r'_{CH} = 2.975 \text{ \AA}$  and  $\theta = 0^\circ$ , and the transition state lies in the vicinity of the nitrogen atom (i.e., in terms of Diagram 1, it is located at  $r_{NH} \approx 3 \text{ \AA}$  and  $\theta \approx 90^\circ$ ). The binding energy for the colinear CN<sup>-</sup>...H-CH<sub>3</sub> arrangement(1) is calculated to be 1.77 kcal/mol before correcting the basis set superposition error (BSSE) [4,7], and 1.69 kcal/mol once the BSSE is corrected using the full counterpoise method [8]. The binding energy for the colinear NC<sup>-</sup>...H-CH<sub>3</sub> arrangement (2) is calculated to be 1.44 kcal/mol before the BSSE correction, and 1.24 kcal/mol with the BSSE corrected. The transition state was accurately located on the potential

energy surface by carrying out analytical second derivatives calculations with the 6-31++G(d,p) basis set at the SCF level. This search locates the transition state at  $r_{\text{NH}} = 3.030 \text{ \AA}$  and  $\theta = 76.76^\circ$  in terms of Diagram 1. The transition state is primarily described as a variation on the angle  $\theta$ . The hessian matrix has one very small negative eigenvalue (-0.0016) in agreement with the very flat potential energy surface near the transition state. The transition state is 0.7 kcal/mol higher in energy than the optimum  $\text{CN} \cdots \text{H-CH}_3$  arrangement (1), and 0.4 kcal/mol higher than the optimum  $\text{NC} \cdots \text{H-CH}_3$  arrangement (2). Thus, the  $\text{CN} \cdots$ methane complex is weakly bound with two colinear minimum energy arrangements. Its binding energy is much smaller than those of the  $\text{CN} \cdots \text{HF}$  and  $\text{CN} \cdots \text{H}_2\text{O}$  complexes (the experimental values are 21.1 and 12.7 kcal/mol, respectively [9]). The potential energy surface is very close to spherical and very flat in the vicinities of the colinear minima.

The effect of correlation energy on the SCF potential energy surface has been studied at the MP2 level using the 6-31++G(d,p) basis set. Figure 2a shows the variation of the energy of the colinear arrangement 1 as a function of  $r_{\text{NH}}$  at the SCF and MP2 levels, and Figure 2b that calculated as a function of the angle  $\theta$  (with the  $r_{\text{NH}}$  distance fixed at the optimum MP2 value of 2.489  $\text{\AA}$ ). Figure 2 shows that the inclusion of correlation energy, which accounts for the dispersion component of the interaction energy, increases the interaction energy: the binding energy changes from 1.77 kcal/mol at the SCF level to 2.54 kcal/mol at the MP2 level (which become 1.69 and 2.07 kcal/mol, respectively, once the BSSE is corrected). Furthermore, the MP2 energy depends less on the angular variations than does the SCF energy. Though not shown, similar results are found for 2.

To show that our findings obtained using the frozen fragment geometries remain valid when the geometries are relaxed, we performed a full optimization of the geometry of the complex 1 at the SCF and MP2 levels with the 6-31++G(d,p) and 6-31++G(2d,2p) basis sets. Table 1 lists the optimized geometrical parameters and the total energies of the  $\text{NC} \cdots \text{H-CH}_3$  arrangement (1) and its fragments. Table 2 gives similar results for the  $\text{CN} \cdots \text{H-CH}_3$  arrangement (2). It is clear from Table 1 and 2 that the geometries and binding energies are not strongly affected either by the geometry relaxation or by the basis set employed. However, at the MP2 level, both minima have shorter interfragment distances and become more stable. Therefore, use of frozen fragments seems to be a good starting approximation in the computation of C-H-anion interactions in general.

## 2) Binding energy

In the previous section, the  $\text{CN}$ -methane complex was found to be bound. We now calculate the binding energies of the two minimum colinear arrangements accurately by employing extensive basis sets, which include the near Hartree-Fock limit basis set [10s7p3d/7s2p] of Lee and Shaeffer [10]. In our SCF and MP2 calculations with those basis sets, the fragment geometries were frozen but the interfragment distances  $r_{\text{NH}}$  and  $r'_{\text{CH}}$  were optimized. At the computed minima, the binding energies with and without counterpoise correction of the BSSE ( $D_{\text{e,CP}}$  and  $D_{\text{e}}$ , respectively) are calculated. The values of the harmonic stretching vibrational frequencies ( $\omega$ ) of the  $\text{CN} \cdots \text{methane}$  complex, computed assuming that the fragments behave as two pseudoparticles, are also calculated. The  $D_{\text{e}}$ ,  $D_{\text{e,CP}}$ , and  $\omega$

values for each basis set studied are included in Table 3 for the linear  $\text{CN} \cdots \text{H}-\text{CH}_3$  arrangement (1), and Table 4 for the linear  $\text{NC} \cdots \text{H}-\text{CH}_3$  arrangement (2).

Table 3 shows that the [10s7p3d/7s2p] basis set presents a negligible BSSE at the SCF level. At the MP2 level, the BSSE error is slightly larger, as expected [4]. Table 3 also shows that the BSSE's in both the SCF and MP2 methods generally become smaller as the basis set quality is increased. The difference between  $D_e$  and  $D_{e,CP}$  (i.e., the BSSE) can be a measure of the error caused by the incompleteness of the basis set employed, one of the two components of the BSSE [7]. At the MP2 level, the BSSE for the near Hartree-Fock basis set is about 0.1 kcal/mol. Therefore, the best estimate of the MP2 binding energy of the  $\text{CN} \cdots \text{H}-\text{CH}_3$  arrangement is  $2.6 \pm 0.1$  kcal/mol. With the same basis set, the best estimate of the SCF binding energy of the same system is  $1.75 \pm 0.01$  kcal/mol. The MP2 binding energy is about 50% larger than the SCF binding energy.

It is interesting to note from Table 3 that the average values of  $D_e$  and  $D_{e,CP}$  obtained with the 6-31++G(2d,2p) and 6-311++G(2d,2p) basis sets are similar to the corresponding values obtained with the near Hartree-Fock basis set at the SCF and MP2 levels. On the basis of this observation and Table 4, the best estimates of the SCF and MP2 binding energies for the  $\text{NC} \cdots \text{H}-\text{CH}_3$  arrangement are 1.34 and 2.3 kcal/mol, respectively.

The zero point corrections for these binding energies can be obtained from the stretching frequencies  $\omega$  assuming that the zero point energies of the fragments remain constant in the complex. Then, at the MP2 level, the zero point corrected binding energies of the  $\text{CN} \cdots \text{H}-\text{CH}_3$  and  $\text{NC} \cdots \text{H}-\text{CH}_3$  arrangements are estimated to be 2.5 and 2.1 kcal/mol, respectively.

Finally, notice from Table 3 that, with the smallest basis set employed, i.e., the 6-31++G(d,p), the  $D_{e,CP}$  value deviates more from the best estimate of the binding energy than does the  $D_e$  value. As this example shows, the  $D_{e,CP}$  values not always are better estimates for the true binding energies than are the corresponding  $D_e$  values.

### 3) Vibrational analysis

In order to justify the validity of the simplified zero point corrections for the two minimum energy colinear arrangements of the  $\text{CN}^- \cdots \text{methane}$  complex, we carried out full vibrational analyses of the two arrangements at their fully optimized geometries using the SCF and MP2 methods with the 6-31++G(d,p) basis set. The harmonic vibrational frequencies, and infrared intensities of all the vibrational modes computed for the monomers and the  $\text{CN}^- \cdots \text{H-CH}_3$  arrangement are included in Table 5, and those for the  $\text{NC}^- \cdots \text{H-CH}_3$  arrangement in Table 6.

Tables 5 and 6 show the existence of two types of vibrations for each arrangement. The lowest five vibrational modes are intermolecular (interfragment) in nature and fall within the far-infrared region of the spectrum ( $10-350 \text{ cm}^{-1}$ ), as expected from the magnitude of the binding energy of the arrangement [11]. The other vibrations, which occur at much higher frequencies, are intramolecular (intrafragment) in nature because they have a one-to-one correspondence with the modes present in the isolated fragments (except for some split and small shift).

In Table 5, the  $A_1$  mode with SCF frequency of  $82 \text{ cm}^{-1}$  corresponds to the  $\nu_\sigma$  stretching [12] between the  $\text{CN}^-$  and  $\text{CH}_4$  fragments, and the two  $E$

modes of SCF frequency  $25\text{ cm}^{-1}$  correspond to the two  $\nu_\beta$  [12] degenerate angular deformations of the  $\text{CN}^-$  fragment relative to the methane. The corresponding MP2 values for those modes are at  $100$  and  $19\text{ cm}^{-1}$ , respectively. The SCF  $A_1$  stretching frequency of Table 5 ( $82\text{ cm}^{-1}$ ) is almost identical with the corresponding value in Table 3 ( $89\text{ cm}^{-1}$ ) computed with the pseudoparticle approach. The same is also true for the MP2 frequencies ( $100\text{ cm}^{-1}$  in the full MP2 vibrational analysis and  $121\text{ cm}^{-1}$  in the pseudoparticle analysis of Table 3). Similar results are found for the  $\text{NC}^- \cdots \text{H-CH}_3$  arrangement:  $65\text{ cm}^{-1}$  in the full vibrational analysis (Table 6) and  $60\text{ cm}^{-1}$  in the pseudoparticle analysis (Table 4). Therefore, the pseudoparticle vibrational analysis provides good estimates of the two  $\nu_\sigma$  stretching frequencies.

Tables 5 and 6 also show that the  $\nu_s$  C-H stretching mode [12] of the two arrangements is red shifted respect to the corresponding value of  $\text{CH}_4$  by about  $30\text{ cm}^{-1}$  at the SCF and MP2 levels. Although the shift is small, it is well within the  $10\text{-}150\text{ cm}^{-1}$  range observed for the complexes of alkynes and alkenes with molecules containing second and third row heteroatoms [13]. This red shift is characteristic of a very weak hydrogen bond [11].

The SCF and MP2 frequencies of all the systems studied here are very similar, except for the C-N stretching which presents a change of about  $400\text{ cm}^{-1}$ . The intensities of the vibrational modes are also similar at SCF and MP2 values, except for some of the  $A_1$  modes and the  $\Sigma_g$  vibration of the  $\text{CN}^-$  fragment. Though not shown, the  $6\text{-}31++\text{G}(2\text{d},2\text{p})$  basis set leads to results similar to those obtained with the  $6\text{-}31++\text{G}(\text{d},\text{p})$  basis set.

### Concluding remarks

Using the SCF and MP2 methods we have shown that the CN<sup>-</sup>...methane complex is bound, with two minima corresponding to the linear CN<sup>-</sup>...H-CH<sub>3</sub> and NC<sup>-</sup>...H-CH<sub>3</sub> arrangements. At the MP2 level, with the zero point energy correction, the binding energy of these two structures are estimated to be  $2.5 \pm 0.1$  and  $2.1 \pm 0.1$  kcal/mol, respectively. Full vibrational analyses of both arrangements show a red shift of about  $30 \text{ cm}^{-1}$  for the  $\nu_s \text{ C-H}$  stretching.

### Acknowledgments

Work at North Carolina State University and Argonne National Laboratory is supported by the U. S. Department of Energy, Basic Energy Sciences, Division of Materials Science, under Grant DE-FG05-86ER45259 and Contract W-31-109-ENG-38, respectively. We express our appreciation for computing time on the ER-Cray computer made available by DOE, and on the VAX-8700 at Argonne National Laboratory provided by the Chemistry Division. J.J.N. thanks NATO and Ministerio de Educacion y Ciencia (Spain) for Fellowships which made it possible to visit North Carolina State University, and CICYT PB89-0268.

## References

1. T. J. Lee, J. Am. Chem. Soc., 111 (1989) 7362.
2. (a) J. M. Williams, H. H. Wang, T. J. Emge, U. Geiser, M. A. Beno, K. D. Carlson, R. J. Thorn, A. J. Schultz, M.-H. Whangbo, Prog. Inorg. Chem., 35 (1987) 51;  
(b) M.-H. Whangbo, D. Jung, J. Ren, M. Evain, J. J. Novoa, F. Mota, S. Alvarez, J. M. Williams, M. A. Beno, A. M. Kini, H. H. Wang, J. R. Ferraro, in "The Physics and Chemistry of Organic Superconductors", G. Saito and S. Kagoshima, eds., (Springer Verlag, Berlin, 1990);  
(c) J. J. Novoa, M.-H. Whangbo, and J. M. Williams, Mol. Cryst. Liq. Cryst., 181 (1990) 25;  
(d) M.-H. Whangbo, J. J. Novoa, D. Jung, J. M. Williams, A. M. Kini, H. H. Wang, U. Geiser, M. A. Beno, and K. D. Carlson, in "Organic Superconductivity", V. Z. Kresin and W. A. Little, eds., (Plenum Press, New York, 1990, page 243).
3. T. Clark, J. Chandrasekhar, G. W. Spitznagel, and P. von R. Schleyer, J. Comput. Chem., 4 (1983) 294.
4. J. H. van Lenthe, J. C. C. M. van Duijneveldt-van der Rijdt, and F. B. van Duijneveldt, in "Ab Initio Methods in Quantum Chemistry", vol II, K. P. Lawley (ed.), (John Wiley, New York, 1987);

5. GAUSSIAN-86, M. J. Frish, J. S. Binkley, H. B. Schlegel, K. Ragavachari, C. F. Melius, R. L. Martin, J. H. P. Stewart, F. W. Boborowicz, C. M. Rohfling, L. R. Kahn, D. J. Defrees, R. Seeger, R. A. Whiteside, D. J. Fox, E. M. Fleuder, J. A. Pople, (Carnegie-Mellon, Quantum Chemistry Publishing Unit, Pittsburg, 1984).
6. The geometry of the fragments was taken to be, see 1 and 2 for definitions:  $r_{CN} = 1.162 \text{ \AA}$ ,  $r_{CH} = 1.091 \text{ \AA}$ ,  $\angle HCH = 109.47^\circ$ .
7. (a) B. Liu and A. D. MacLean, J. Chem. Phys., 59 (1973) 4557;  
(b) B. Liu and A. D. MacLean, J. Chem. Phys., 91 (1989) 2348.
8. S. F. Boys and F. Bernardi, Mol. Phys., 19 (1970) 553.
9. (a) J. W. Larson and T. B. J. McMahon, J. Am. Chem. Soc., 105 (1983) 2944;  
(b) J. W. Larson, J. E. Szulejko, and T. B. J. McMahon, J. Am. Chem. Soc., 110 (1988) 7604.
10. T. J. Lee and H. F. Schaeffer, J. Chem. Phys., 83 (1985) 1784.
11. R. J. Saykally, Acc. Chem. Res., 9 (1989) 295.
12. G. C. Pimentel and A. L. McClellan, "The Hydrogen Bond", (W. H. Freeman, San Francisco, 1960), pag. 68.
13. (a) M. H. Jeng and B. S. Ault, J. Phys. Chem., 94 (1990) 1323;  
(b) M. H. Jeng and B. S. Ault, J. Phys. Chem., in press.

14. K. Nakamoto, "Infrared Spectra of Inorganic and Coordination Compounds" (John Wiley, New York, 1963).

**Table 1**

Optimized geometry (in Å and degrees) and total energy (E, in a.u.) for the CN<sup>-</sup>...H-CH<sub>3</sub> (1) arrangement and its fragments computed at the SCF and MP2 levels using the 6-31++G(d,p) and 6-31++G(2d,2p) basis sets. The dissociation energy of the complex (D<sub>e</sub>, in kcal/mol) is also included.

	SCF		MP2	
	6-31++G(d,p)	6-31++G(2d,2p)	6-31++G(d,p)	6-31++G(2d,2p)
<b>CN<sup>-</sup></b>				
r <sub>CN</sub>	1.162	1.158	1.201	1.196
E	-92.314872	-92.319323	-92.603403 <sup>a</sup>	-92.626304 <sup>a</sup>
<b>CH<sub>4</sub></b>				
r <sub>CH</sub>	1.084	1.083	1.085	1.086
∠HCH	109.47	109.47	109.47	109.47
E	-40.202169	-40.204253	-40.366110 <sup>a</sup>	-40.380388 <sup>a</sup>
<b>CN...CH<sub>4</sub></b>				
r <sub>NH</sub>	2.630	2.634	2.478	2.387
θ	0.	0.	0.	0.
r <sub>CN</sub>	1.162	1.158	1.200	1.195
r <sub>CH</sub>	1.086	1.085	1.088	1.088
∠HCH	109.83	109.86	108.85	109.87
E	-132.519850	-132.526376	-132.973464 <sup>a</sup>	-133.011200 <sup>a</sup>
D <sub>e</sub>	1.76	1.76	2.48	2.82

<sup>a</sup> From a frozen core MP2 calculation.

**Table 2**

Optimized geometry (in Å and degrees) and total energy (E, in a.u.) for the NC<sup>-</sup>...H-CH<sub>3</sub> arrangement computed at the SCF level using the 6-31++G(d,p), 6-31++G(2d,2p), and 6-311++G(2d,2p) basis sets. The dissociation energy of the complex (D<sub>e</sub>, in kcal/mol) is also included.

	6-31++G(d,p)	6-31++G(2d,2p)	6-311++G(2d,2p)
r <sub>NH</sub>	2.958	2.985	2.958
θ	0.	0.	0.
r <sub>CN</sub>	1.161	1.158	1.162
r <sub>CH</sub>	1.085	1.085	1.091
∠HCH	109.76	109.77	108.50
E	-132.519290	-132.525816	-132.552832
D <sub>e</sub>	1.41	1.41	1.61

**Table 3**

Optimized interfragment distance ( $r_{NH}$ , in Å), total energy (E, in a.u.), dissociation energy ( $D_e$ , in kcal/mol), BSSE corrected dissociation energy ( $D_{e,CP}$ , in kcal/mol), and stretching frequency ( $\omega$ , in  $\text{cm}^{-1}$ ) computed with various basis sets at the SCF and MP2 levels for the colinear arrangement  $\text{CN}^- \cdots \text{H-CH}_3$  (1), and with frozen fragment geometries.

Basis set			$r_{NH}$	E	$D_e$	$D_{e,CP}$	$\omega$
6-31++G(d,p)	SCF	2.652	-132.519772	1.77	1.69	89	
	MP2	2.489	-132.970447 <sup>a</sup>	2.54	2.07	121	
6-31++G(2d,2p)	SCF	2.655	-132.526245	1.80	1.66	90	
	MP2	2.439	-133.008862 <sup>a</sup>	2.91	2.31	113	
6-311++G(2d,2p)	SCF	2.672	-132.553061	1.75	1.71	91	
	MP2	2.451	-133.052454 <sup>a</sup>	2.83	2.45	114	
[10s7p3d/7s2p]	SCF	2.670	-132.565330	1.75	1.74	91	
	MP2	2.457	-133.085646 <sup>a</sup>	2.76	2.63	116	

<sup>a</sup> From a frozen core MP2 calculation.

**Table 4**

Optimized interfragment distance ( $r'_{\text{CH}}$ , in Å), total energy (E, in a.u.), dissociation energy ( $D_e$ , in kcal/mol), BSSE corrected dissociation energy ( $D_{e,CP}$ , in kcal/mol), and stretching frequency ( $\omega$ , in  $\text{cm}^{-1}$ ) computed with various basis sets at the SCF and MP2 levels for the colinear arrangement  $\text{NC}\cdots\text{H-CH}_3$  (2), and with frozen fragment geometries.

Basis set		$r'_{\text{CH}}$	E	$D_e$	$D_{e,CP}$	$\omega$
6-31++G(d,p)	SCF	2.975	-132.519192	1.44	1.24	60
	MP2	2.770	-132.969906 <sup>a</sup>	2.20	1.74	77
6-31++G(2d,2p)	SCF	3.004	-132.525663	1.43	1.29	63
	MP2	2.737	-133.007990 <sup>a</sup>	2.35	1.96	74
6-311++G(2d,2p)	SCF	3.001	-132.552437	1.36	1.33	63
	MP2	2.678	-133.051812	2.43	2.17	102

<sup>a</sup> From a frozen core MP2 calculation.

Table 5

Symmetry, frequency ( $\omega$ , in  $\text{cm}^{-1}$ ), and infrared intensity (I, in  $\text{kM/mol}$ ) of the normal modes calculated at the SCF and MP2 levels with the 6-31++G(d,p) basis set for the minimum  $\text{CN} \cdots \text{H-CH}_3$  arrangement (1) and its fragments. The experimental value of the frequency, when available, is also given for comparison.

Symmetry	SCF		MP2		Expt.
	$\omega$	I	$\omega$	I	$\omega$
$\text{CN}^-$					
$\Sigma_g$	2330	48	1991	3	2080-2239 <sup>a</sup>
$\text{CH}_4$					
$\text{T}_2$	1463	12	1397	15	1357 <sup>a</sup>
$\text{E}$	1673	0	1594	0	1573 <sup>a</sup>
$\text{A}_1$	3169	0	3122	0	3143 <sup>a</sup>
$\text{T}_2$	3276	43	3269	23	3154 <sup>a</sup>
$\text{CN} \cdots \text{H-CH}_3$					
$\text{E}$	25	0	19	1	
$\text{A}_1$	82	24	100	25	
$\text{E}$	163	0	152	0	
$\text{A}_1$	1431	7	1360	9	
$\text{E}$	1485	10	1419	11	
$\text{E}$	1680	1	1599	2	
$\text{A}_1$	2331	59	1993	5	
$\text{A}_1$	3143	51	3089	69	
$\text{E}$	3243	83	3235	51	
$\text{A}_1$	3273	5	3246	24	

<sup>a</sup> Reference [14]

**Table 6**

Symmetry, frequency ( $\omega$ , in  $\text{cm}^{-1}$ ), and infrared intensity (I, in  $\text{kM/mol}$ ) of the normal modes calculated at the SCF level with the 6-31++G(d,p) basis set for the minimum  $\text{NC}\cdots\text{H-CH}_3$  arrangement (2).

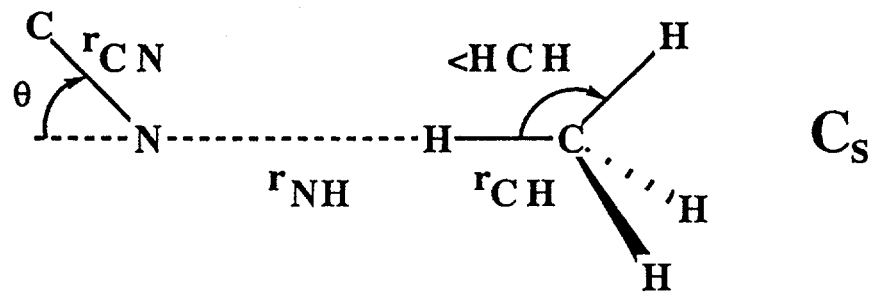
Symmetry	$\omega$	I
<b><math>\text{NC}\cdots\text{CH}_4</math></b>		
E	28	2
$A_1$	65	21
E	154	1
$A_1$	1434	8
E	1483	10
E	1679	1
$A_1$	2335	47
$A_1$	3148	37
E	3248	77
$A_1$	3275	0

**Figure captions****Figure 1.**

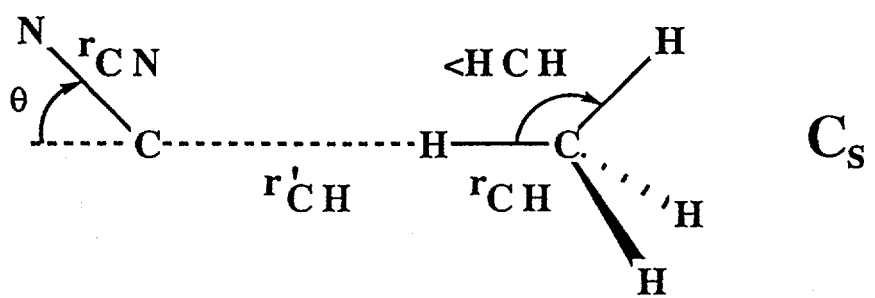
Potential energy surface computed at the SCF level with the 6-31++G(d,p) basis set for (a) the CN $\cdots$ H-CH<sub>3</sub> arrangement (1), (b) the NC $\cdots$ H-CH<sub>3</sub> arrangement (2), and (c) the CN $\cdots$ methane arrangement 3. The values of  $r_1$  and  $r_2$  (both in Å) in (a) are defined as  $r_1 = r_{\text{NH}} \cdot \cos\theta$  and  $r_2 = r_{\text{NH}} \cdot \sin\theta$ , and those in (b) are defined as  $r_1 = r'_{\text{CH}} \cdot \cos\theta$ , and  $r_2 = r'_{\text{CH}} \cdot \sin\theta$ . The values of the contours plotted (in kcal/mol) are indicated at the right-hand-side margin. The values are those encountered moving away from the minimum. The energies given respect to the energy of the optimum CN $\cdots$ H-CH<sub>3</sub> arrangement, which is shown in (a) by a the symbol •.

**Figure 2.**

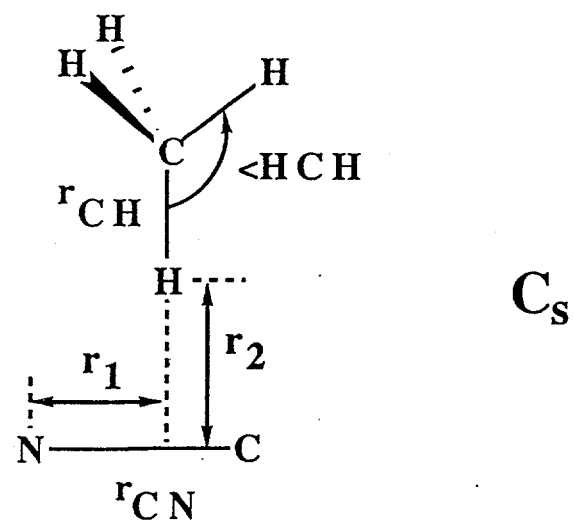
- (a) Energy of the colinear CN $\cdots$ H-CH<sub>3</sub> arrangement (1) as a function of the  $r_{\text{NH}}$ , computed at the SCF and MP2 levels.
- (b) Energy of the CN $\cdots$ H-CH<sub>3</sub> arrangement (1) as a function of the angle  $\theta$ , computed at the SCF and MP2 levels, with the  $r_{\text{NH}}$  distance fixed at the optimum MP2 value of 2.489 Å.



1

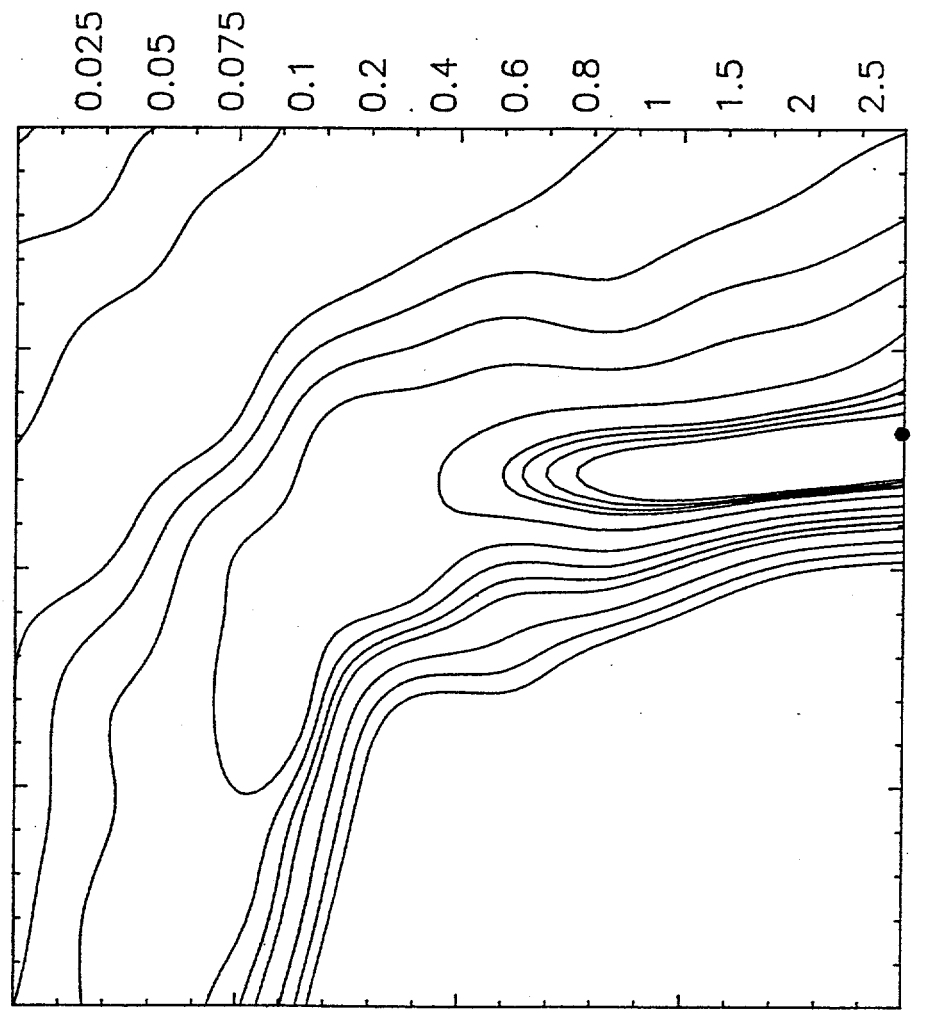


2



3

C-N(−)...H-CH<sub>3</sub>



0

r<sub>1</sub>

4

r<sub>2</sub>

4

1. a

Fig

NC(–)...H–CH<sub>3</sub>

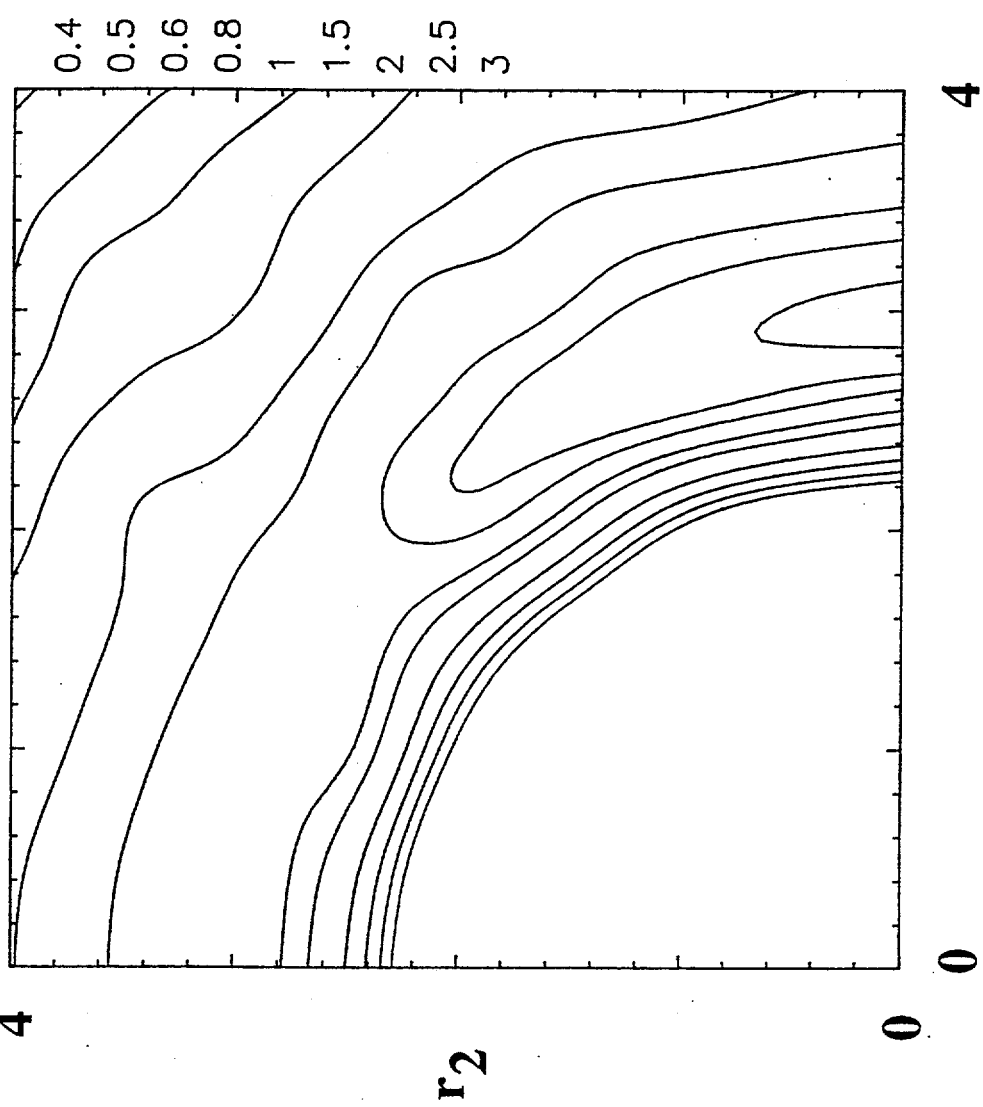


Fig 1.6

NC(—)...H—CH<sub>3</sub>

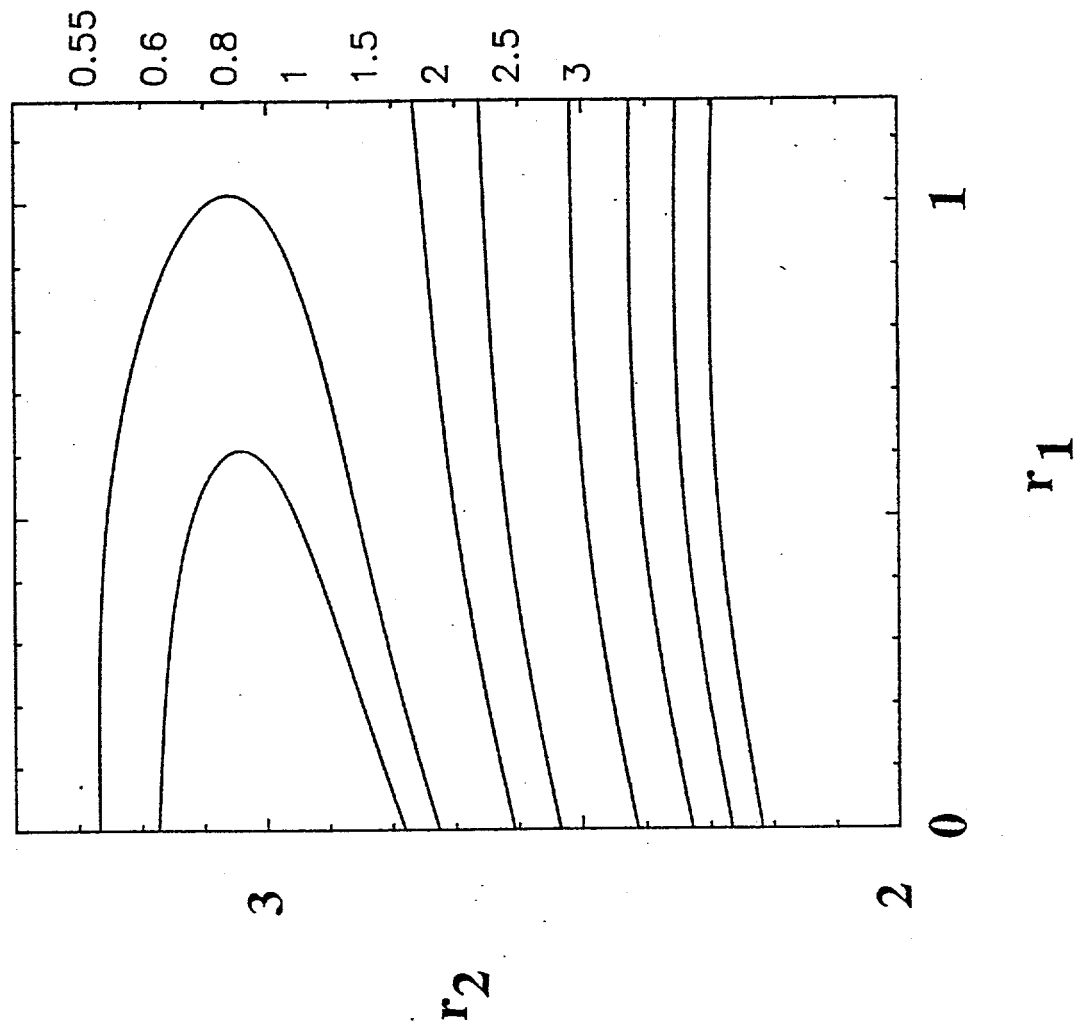


Fig 4.c

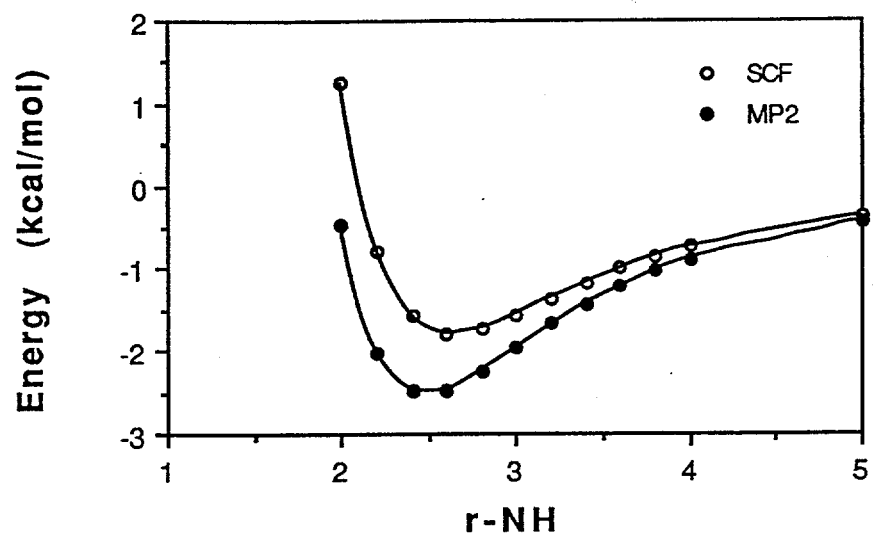


Fig 2.a

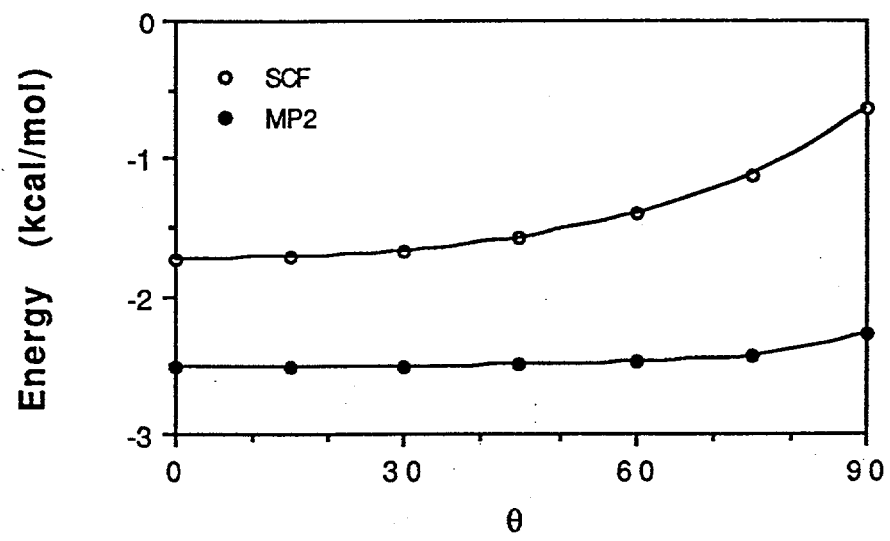


Fig 2.6.